


N. KUMARI  
S.B. KRUPANIDHI  
K.B.R. VARMA 

# Structural, ferroelectric and optical properties of $\text{Bi}_2\text{VO}_{5.5}$ thin films deposited on platinized silicon $\{(100)\text{ Pt}/\text{TiO}_2/\text{SiO}_2/\text{Si}\}$ substrates

Materials Research Center, Indian Institute of Science, Bangalore 560012, India

Received: 26 October 2007/Accepted: 18 March 2008  
Published online: 23 April 2008 • © Springer-Verlag 2008

**ABSTRACT** Bismuth vanadate ( $\text{Bi}_2\text{VO}_{5.5}$ , BVO) thin films have been deposited by a pulsed laser ablation technique on platinized silicon substrates. The surface morphology of the BVO thin films has been studied by atomic force microscopy (AFM). The optical properties of the BVO thin films were investigated using spectroscopic ellipsometric measurements in the 300–820 nm wavelength range. The refractive index ( $n$ ), extinction coefficient ( $k$ ) and thickness of the BVO thin films have been obtained by fitting the ellipsometric experimental data in a four-phase model (air/BVO<sub>rough</sub>/BVO/Pt). The values of the optical constants  $n$  and  $k$  that were determined through multi-layer analysis at 600 nm were 2.31 and 0.056, respectively. For fitting the ellipsometric data and to interpret the optical constants, the unknown dielectric function of the BVO films was constructed using a Lorentz model. The roughness of the films was modeled in the Bruggmann effective medium approximation and the results were compared with the AFM observations.

PACS 78.20.-e; 77.84.-s; 77.55.+f

## 1 Introduction

The study of ferroelectric thin films has received much attention owing to their applications in integrated circuit memories, optical waveguides and pyroelectric imaging sensors [1–7]. Thin-film-based infrared detectors and focal plane arrays are expected to yield better sensitivity and faster response than their ceramic and bulk single crystal counterparts, and could be deposited directly on silicon readout circuitry [8–10]. The ferroelectric materials belonging to the family of Aurivillius phases have been of considerable interest for a variety of integrated device applications such as non-volatile memories, optical memories and piezoelectric and electro-optic devices [11–14]. This family has the general chemical formula  $(\text{Bi}_2\text{O}_2)^{2+}(\text{A}_{n-1}\text{B}_n\text{O}_{3n+1})^{2-}$ , in which A represents mono-, di- or tri-valent ions or a mixture thereof, B represents tetra-, penta- or hexa-valent ions of the perovskite structure and  $n$  is the number of perovskite blocks sandwiched between  $(\text{Bi}_2\text{O}_2)$  layers [15]. Bismuth vanadate,  $\text{Bi}_2\text{VO}_{5.5}$  (BVO), is a vanadium analogue of an  $n = 1$  mem-

ber of the Aurivillius family of oxides and has been found to be ferroelectric below 725 K [16–20]. The optical properties of ferroelectric materials are of special interest for applications in uncooled infrared detectors, optical sensors and waveguides [21–24]. Though the optical properties of sputtered BVO thin films have been studied by transmittance measurements [25], because of their potential applications, investigations of the details with regard to the effects of the film thickness, crystal structure, orientation of the crystallites, crystallite-size distribution, packing density, the nature of the bottom electrode and the morphology of the film surface are in order.

It is worth investigating the structure–optical property correlation in BVO films due to their potential in optical applications. Therefore, spectroscopic ellipsometry, which needs no reference sample for calibration and measures two independent parameters (the ellipsometric angles  $\Psi$  and  $\Delta$ , where  $\tan \Psi$  measures the ratio of the moduli of the amplitudes of reflection and  $\Delta$  is the phase difference between p- and s-polarized reflected light) at each wavelength, is one of the most adapted measuring methods to analyze the multilayer structure.

In this article, we report the fabrication details of ferroelectric  $\text{Bi}_2\text{VO}_{5.5}$  thin films on platinized silicon  $\{(100)\text{ Pt}/\text{TiO}_2/\text{SiO}_2/\text{Si}\}$  substrates by pulsed laser deposition and their structural and optical properties investigated by spectroscopic ellipsometry in the wavelength range of 300–850 nm. A parameterized relaxed Lorentz formula was employed to describe the dielectric function of the BVO films, and assuming a four-layer model (ambient/rough BVO/BVO/Pt) for BVO on platinized silicon substrates the ellipsometric data were analyzed. The roughness of the BVO films was modeled according to the Bruggmann effective medium approximation (EMA) and is also compared with atomic force microscopy (AFM) studies. A good fit of the model to measured  $\Psi$  and  $\Delta$  data of spectroscopic ellipsometry has been obtained and the optical constants are calculated.

## 2 Experimental

### 2.1 Thin-film preparation and structural characterizations

The ferroelectric thin films of BVO for the present studies were grown by a pulsed laser ablation technique

on platinized silicon substrates having the configuration Pt(100)/TiO<sub>2</sub>/SiO<sub>2</sub>/Si(100). The laser used for BVO thin-film deposition was a KrF (Lambda Physik Compex 201, wavelength 248 nm) excimer with 5-Hz repetition frequency and 10-ns pulse duration. The output laser beam was focused onto a rotating target at an angle of 45° by a UV lens with a focal length of 30 cm. The stability of the incoming beam was monitored using an external energy meter. Laser energy of 160 mJ/pulse was maintained constant during the deposition and the laser beam was focused to obtain a fluence of approximately 2.5 J cm<sup>-2</sup> for all the samples under study. A sintered target, produced from a mixture of high-purity Bi<sub>2</sub>O<sub>3</sub> and V<sub>2</sub>O<sub>5</sub> oxides (Aldrich, purity 99.9%) in appropriate quantities to ensure the stoichiometric composition Bi<sub>2</sub>VO<sub>5.5</sub> was used for deposition. The BVO target was fabricated from the fine powders obtained by ball milling of Bi<sub>2</sub>O<sub>3</sub> and V<sub>2</sub>O<sub>5</sub> in stoichiometric ratio. Initially the ball-milled powders were calcined at 800 °C for 8 h. The calcined powder was then pressed at 80-kN force in a 18-mm circular die and the pressed pellets were sintered at 825 °C for 5 h. The target was freshly polished prior to each deposition to produce a uniform plasma cloud and mounted on a motor-driven shaft. Before deposition, the chamber was initially evacuated to 1 × 10<sup>-6</sup> mbar and the films were deposited under various oxygen partial pressures in the range of 20–100 mTorr. Stoichiometric growth during the deposition process was ensured by a controlled oxygen flow into the deposition chamber. The flow of high-purity oxygen was regulated by a mass-flow controller, which allowed maintaining a stable oxygen pressure. During deposition, the substrate temperature was recorded by means of a thermocouple. The substrate was placed parallel to the target at a distance of approximately 4 cm. The substrate temperature during deposition was maintained at 600 to 700 °C in order to achieve good crystallization.

X-ray diffraction (XRD) studies were carried out to ensure the crystalline quality of the BVO films using Cu K<sub>α</sub> ~ 1.541 Å radiation (Scintag XR2000 diffractometer). Microstructural details and the thickness of the films were obtained using a scanning electron microscope (SEM, Sirion 200). The surface morphology of the BVO films was examined by means of an ex situ contact mode atomic force microscope (AFM, Veeco CP-II). The AFM images were obtained in the repulsive-force regime with a force constant of 1.5 nN between the AFM tip and the sample surface.

## 2.2 Electrical characterization

For electrical measurements, gold dots of 1.96 × 10<sup>-3</sup>-cm<sup>2</sup> area were deposited on the top surface of the films through a shadow mask and a thermal evaporation technique. The electrode dots were annealed at 250 °C for 30 min. The Pt coating was used as the bottom electrode for electrical measurements. A HP4294A impedance analyzer was used for the conventional dielectric measurements in the 100 Hz–100 kHz frequency range at a signal strength of 0.5 V. The polarization–electric field (*P*–*E*) hysteresis and pulsed polarization (PUND, positive up negative down) phenomenon were studied at room temperature using a precision workstation (Radiant Technologies, Inc.) ferroelectric test system in virtual ground mode.

## 2.3 Spectroscopic ellipsometry measurements

Spectroscopic ellipsometry measurements for BVO thin films on platinized silicon substrates were carried out at room temperature in the 0.75–4.0 eV (ultraviolet–visible) photon energy range using a computer-controlled variable angle of incidence spectroscopic ellipsometer (SENTECH 850, SENTECH Instruments) of the rotating polarizer and analyzer type in which these rotate at a speed ratio of 1 : 1. The optical constants of the BVO films were determined by fitting the model function to the measured data using the SpectraRay2-5656b software package (SENTECH Instruments).

## 3 Results and discussion

### 3.1 Structural characterization

**3.1.1 X-ray diffraction study.** The X-ray diffraction pattern obtained for BVO thin films deposited on a Pt/TiO<sub>2</sub>/SiO<sub>2</sub>/Si substrate at 650 °C under 100 mTorr oxygen partial pressure is depicted in Fig. 1. All the diffraction peaks in this figure match well with those of bulk bismuth vanadate layered perovskite structure and no secondary phase formation has been noticed. The diffraction pattern has been indexed on the basis of an orthorhombic structure (JCPDS 42-0135). The lattice parameters obtained from this pattern are in close agreement with those reported for the bulk BVO. However, the pattern suggests the presence of a preferred texture in these films. The selective strong and sharp Bragg peaks (002), (004) and (006) indicate that the pulsed laser ablation-grown films were textured and possessed a high degree of crystallinity with preferred *c*-axis orientation. The extent of texture in the grain-oriented films was obtained by a semiquantitative method using Lotgering's factor [26], where the degree of grain orientation *f* is given by

$$f = \frac{p - p_0}{1 - p_0}, \quad (1)$$

where  $p = \Sigma I_{00l} / \Sigma I_{hkl}$  for the given oriented sample and  $p_0 = \Sigma I_{00l} / \Sigma I_{hkl}$  for the non-oriented sample, which in our

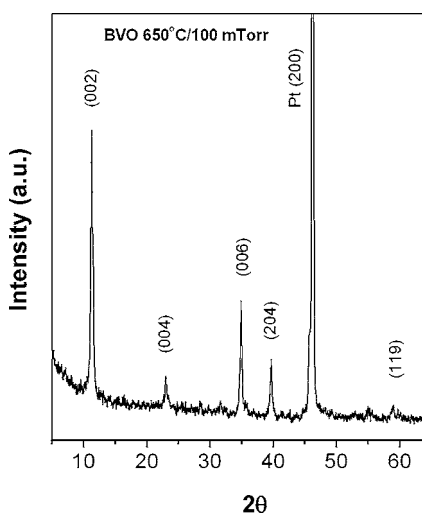


FIGURE 1 XRD pattern of Bi<sub>2</sub>VO<sub>5.5</sub> thin film deposited at 650 °C

study was calculated from the BVO bulk X-ray diffraction studies. Here,  $I_{hkl}$  and  $I_{00l}$  are the intensities of the ( $hkl$ ) and ( $00l$ ) peaks, respectively. An orientation factor of 0.83 as obtained by the above formula suggests that the films were highly oriented. This implies that a relatively greater number of grains with ( $00l$ ) planes parallel to the film surface exists in these films. The preferential orientation of the films is due to the strong anisotropy associated with the structure of the Aurivillius family of oxides. The free energy for the growth along the  $c$  axis could be a minimum and as a result the growth is dominant along this axis. The orthorhombic distortion ( $b/a$ ) of the present film was lower than the reported values for the bulk.

**3.1.2 Microstructure and surface morphology.** Surface and cross-sectional microstructures of the BVO thin films deposited on platinized silicon surfaces were recorded by a scanning electron microscope. Figure 2a and b show the surface and cross-sectional scanning electron micrographs of the BVO thin films, respectively. It is observed that the BVO films consist of closely packed rod-shaped grains around  $0.3\text{--}0.35\ \mu\text{m}$  in width and several nanometers in length. The cross-sectional SEM images revealed the presence of densely packed grains across the film. The thickness of the film estimated from the cross-sectional SEM images is around  $325\ \text{nm}$ . Energy dispersive X-ray (EDAX) analysis carried out on the well-crystalline films of BVO has

confirmed the stoichiometric ( $\text{Bi} : \text{V} = 2 : 1$ ) nature of the films.

The surface topography measurements have been performed with an atomic force microscope (AFM) operating in contact mode for BVO thin films and the results obtained are shown in Fig. 3a and b as two-dimensional and three-dimensional micrographs. The AFM micrograph in Fig. 3a shows the surface topography of a BVO thin film containing a homogeneous distribution of grains. The grain size that is determined from the picture lies in the range of  $0.3\text{--}0.35\ \mu\text{m}$ . The AFM micrograph in Fig. 3b shows the three-dimensional image. The root mean square (rms) roughness has been calculated for a  $5 \times 5\ \mu\text{m}^2$  area. The root mean square roughness ( $R_a$ ) lies in the  $10$  to  $12\ \text{nm}$  range. These values of the surface roughness are compared with those obtained from the ellipsometric data analysis discussed later in this paper.

### 3.2 Ferroelectric and dielectric characterization

To ensure the polar nature of the BVO films deposited on platinized silicon substrates, these films were characterized for their ferroelectric and dielectric properties in metal–insulator–metal (MIM) configuration using gold dots of area  $1.96 \times 10^{-3}\ \text{cm}^2$  as the top electrode and the platinum metal serving as the bottom electrode. Figure 4a shows the ferroelectric hysteresis loop of an Au/BVO/Pt capac-

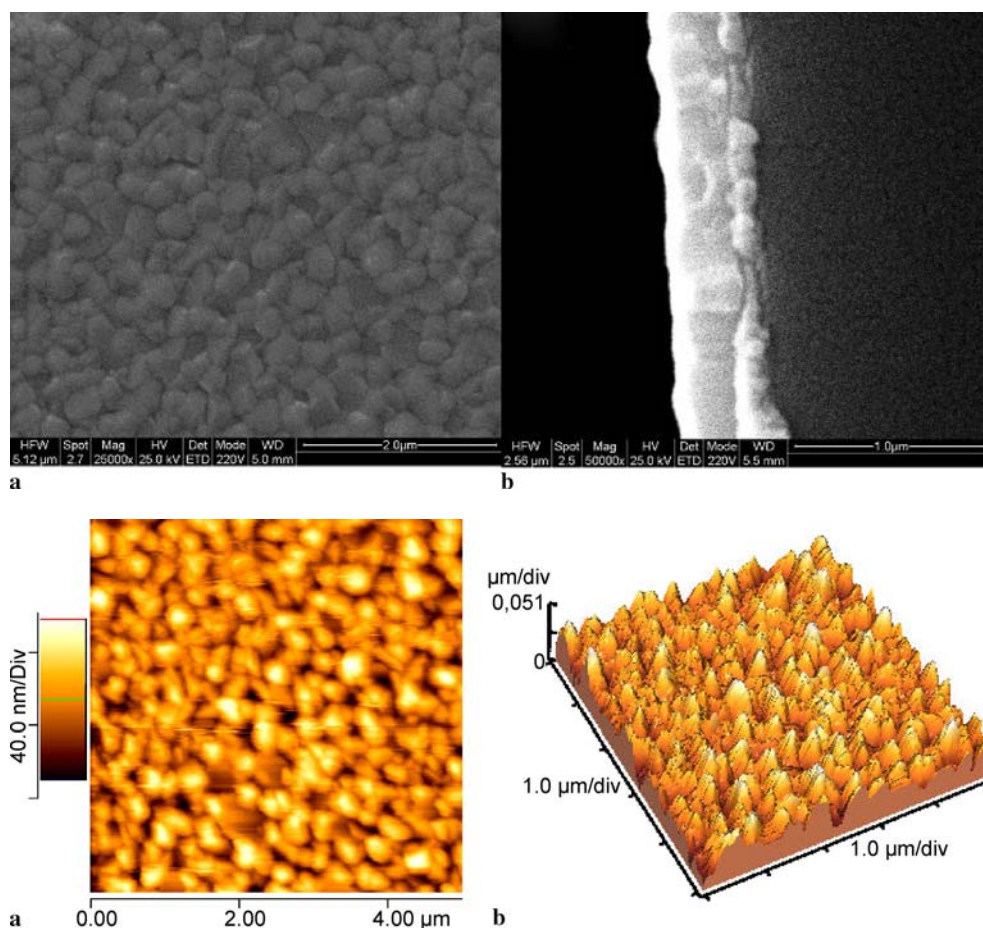


**FIGURE 2** (a) The surface morphology and (b) the cross-sectional SEM view of  $\text{Bi}_2\text{VO}_{5.5}$  thin film

**FIGURE 3** (a)  $5 \times 5\ \mu\text{m}^2$  AFM micrograph showing surface morphology of  $\text{Bi}_2\text{VO}_{5.5}$  thin film. (b) Three-dimensional topography of  $\text{Bi}_2\text{VO}_{5.5}$  thin film. The rms roughness obtained from this image is  $11.92\ \text{nm}$

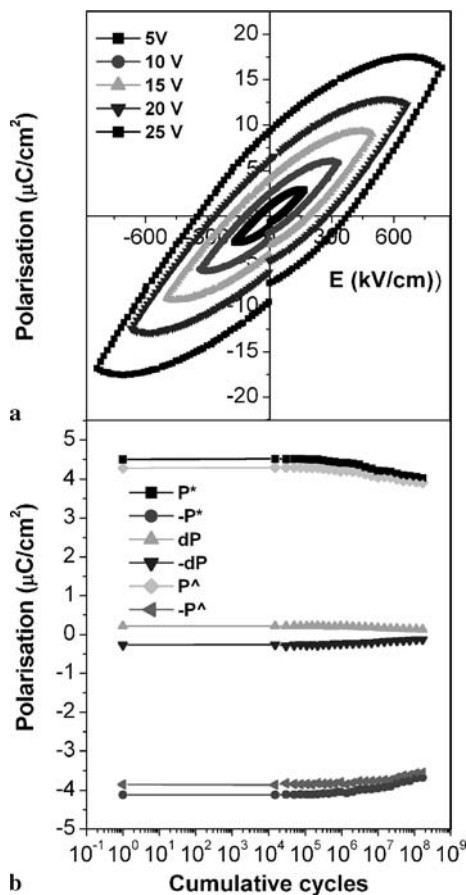


**FIGURE 4** (a) The  $P$ - $E$  hysteresis loop for  $\text{Bi}_2\text{VO}_{5.5}$  thin film. (b) Polarization vs. number of 5 V pulsed voltage cycles applied to Au/BVO/Pt thin-film capacitor

itor measured at various applied voltages ranging from 5 to 25 V. The BVO film is characterized by well-saturated polarization–electric field ( $P$ - $E$ ) switching curves. At the applied voltage of 25 V and the measuring frequency of 1 kHz, the remanent polarization  $P_r$  and the coercive field  $E_c$  are about  $9.3 \mu\text{C}/\text{cm}^2$  and  $365 \text{ kV}/\text{cm}$ , respectively. The value of the coercive field seems to be quite high for storing a charge of this magnitude. It has been explained in our earlier work that this kind of behavior in BVO films on platinized silicon substrates may be due to the high oxide ion conductivities in the low-frequency range [27]. In order to check the fatigue response of the BVO films, the Au/BVO/Pt capacitor was further subjected to a pulsed polarization (PUND) experiment. The PUND measurements were carried out using a 5 V pulsed waveform with a pulse width of 1 ms, and the test capacitor was fatigued with a 5 V, 10 kHz pulsed waveform. The corresponding results are shown in Fig. 4b. The value of the switchable polarization remains almost constant for the initial few cycles. In Fig. 4a,  $P_{\text{max}}$  is about  $3 \mu\text{C}/\text{cm}^2$  and  $P_r$  is about  $1 \mu\text{C}/\text{cm}^2$  for the voltage scan of  $\pm 5 \text{ V}$ . On the other end,  $P^*$  in Fig. 4b is around  $4.4 \mu\text{C}/\text{cm}^2$  and  $dP$  is  $0.2 \mu\text{C}/\text{cm}^2$ . A small difference that we see in  $P^*$  and  $P_{\text{max}}$  values is attributed to the different nature of the waveforms used during the two measurements; for example, in  $PE$  hysteresis measurement, the waveform used was triangular and gives the transient response of the sample, while in PUND

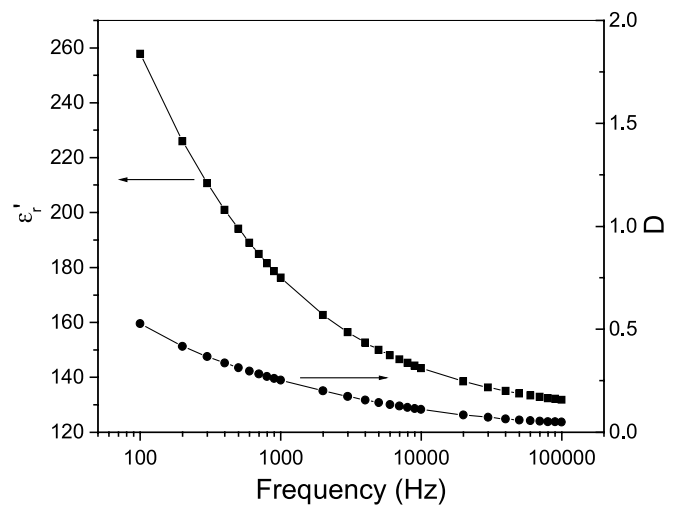


**FIGURE 5** Variation of dielectric constant and loss as a function of frequency for  $\text{Bi}_2\text{VO}_{5.5}$  thin film

measurement a rectangular pulse has been used. The small difference in the polarizations may also arise due to the non-switchable charges in BVO, as pointed out in our earlier work. It has been observed that there is around 10% reduction in the switchable polarization ( $P^*$ ) after  $10^8$  cycles.

Figure 5 shows the variation of the dielectric constant and the dissipation factor as a function of frequency at room temperature. The dispersion observed in the dielectric constant at lower frequency is quite high as compared to that at higher frequency. This lesser dispersion observed at higher frequencies might have its origin in the grains, while at lower frequencies the response is arising from the grain boundaries, free charges and oxide ion vacancies, which lead to strong dispersion. The values of the dielectric constant and the dissipation factor measured at 100 kHz are 130 and 0.04, respectively.

### 3.3 Optical characterization

The BVO thin films were characterized for their optical properties by spectroscopic ellipsometry. Spectroscopic ellipsometry could effectively be used to determine the dielectric function and thickness of a thin-film sample by comparing the measured data with a best-fit model calculation. The standard ellipsometric parameters (angles) measured are defined through  $\Psi$  and  $\Delta$ , where  $\tan \Psi$  measures the ratio of the moduli of the amplitudes of reflection and  $\Delta$  is the phase difference between p- and s-polarized reflected light.  $\Psi$  takes values from 0 to  $90^\circ$  and  $\Delta$  varies from 0 to  $360^\circ$  for a particular experiment carried out. The ellipsometric angles are related to the ratio  $\rho$  of the Fresnel coefficients,  $r_s$  and  $r_p$ , for s- and p-polarizations, respectively [28]:

$$\rho \equiv \frac{r_p}{r_s} = \tan \Psi \exp(i\Delta), \quad (2)$$

where  $\Psi$  and  $\Delta$  are the ellipsometric parameters and are measured directly as azimuthal angles of the analyzer and polarizer at which the light intensity at the detector has a minimum. For the type of instrument used in the present work, the actual quantities measured are  $\Psi$  and  $\Delta$ , from which  $\rho$  is calculated. The dielectric function ( $\epsilon$ ) as well as the refractive index

( $n$ ) and extinction coefficient ( $k$ ) are calculated from  $\rho$  and  $\varphi$  through the relations

$$\varepsilon = (n + ik)^2 = \sin^2 \varphi + \sin^2 \varphi \tan^2 \varphi \frac{(1 - \rho)^2}{(1 + \rho)^2}, \quad (3)$$

where  $\varphi$  is the angle of incidence. The refractive index and extinction coefficient are obtained as follows:

$$n = \frac{1}{2} \sqrt{\sqrt{\varepsilon_1^2 + \varepsilon_2^2} + \varepsilon_1}, \quad (4)$$

$$k = \frac{1}{2} \sqrt{\sqrt{\varepsilon_1^2 + \varepsilon_2^2} - \varepsilon_1}. \quad (5)$$

Here,  $\varepsilon_1$  and  $\varepsilon_2$  are the real and imaginary parts of the complex dielectric function  $\varepsilon$ . The measurement of the ellipsometric quantities  $\Psi$  and  $\Delta$  for all the samples under study was done in air at 70° angle of incidence. We used a parameterized relaxed Lorentz oscillator model to express the optical response of the optical functions of BVO films. In the ultraviolet–visible range, the parameterized relaxed Lorentz oscillator model is very useful for obtaining the dielectric functions of most materials such as dielectrics and metal oxides [29]. The complex dielectric function in the single Lorentz oscillator model is given by

$$\varepsilon = \varepsilon_\infty + \frac{A\lambda^2}{\lambda^2 - B^2 - i2C\lambda}, \quad (6)$$

where  $\varepsilon$  is the complex dielectric function,  $\lambda$  is the measured wavelength (in nm) and  $\varepsilon_\infty$  is the high-frequency dielectric constant. However, most of the fitted values are unitless while  $A$ ,  $B$  and  $C$  are constants. In order to estimate the optical constants of the BVO thin films the ellipsometric data were analyzed by modeling in a multilayer system [28], which is shown in Fig. 6.

Modeling of the measured data was done under the assumption that the film and the substrate are isotropic. The roughness was modeled in the Bruggmann effective medium approximation [30, 31]. The dielectric function  $\varepsilon$  of the BVO films was expressed by a relaxed Lorentz oscillator model. The four-phase-model system consists of air, rough BVO layer, dense BVO layer and platinum layer. In this multilayer system, the platinum layer is so thick that the incident light

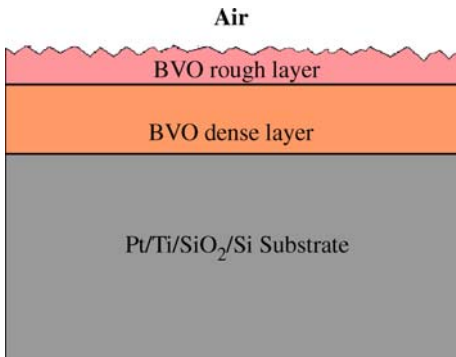


FIGURE 6 The optical model used in the ellipsometric evaluation of optical constants and roughness of a 325-nm-thick Bi<sub>2</sub>VO<sub>5,5</sub> film

could not propagate through. So, the platinized silicon substrate (including the thermal oxide and Ti adhesion layer) can be treated as a single substrate. Variables in the fitting procedure include all the layer thicknesses, the volume fraction of the voids in the rough layer and the dispersion relations describing the optical properties of the BVO films. The optical constants of the BVO films were determined by fitting the model function to the measured data using the SpectraRay2-5656b software package (SENTECH Instruments). The program is based on least-square regression to obtain the unknown fitting parameters and their maximum confidence limit. The procedure is to vary the fitting parameters to minimize the difference between the measured and calculated  $\Psi$  and  $\Delta$  values. The root-mean-square fractional error  $\sigma$ , defined by

$$\sigma^2 = \frac{1}{2N - M} \times \sum_{i=1}^N \left\{ \left( \frac{\psi_i^{\text{mod}} - \psi_i^{\text{exp}}}{\sigma_{\psi,i}^{\text{exp}}} \right)^2 + \left( \frac{\Delta_i^{\text{mod}} - \Delta_i^{\text{exp}}}{\sigma_{\Delta,i}^{\text{exp}}} \right)^2 \right\}, \quad (7)$$

has been used to judge the quality of the fit between the measured and the modeled data and is minimized in the fit. Here,  $N$  is the number of measured  $\Psi$  and  $\Delta$  pairs included in the fit,  $M$  is the number of fit parameters and  $i$  is the summation index. Also,  $\psi_i^{\text{exp}}$ ,  $\Delta_i^{\text{exp}}$  and  $\psi_i^{\text{mod}}$ ,  $\Delta_i^{\text{mod}}$  are the experimental and modeled values of  $\Psi$  and  $\Delta$ , respectively.  $\sigma_{\psi,i}^{\text{exp}}$  and  $\sigma_{\Delta,i}^{\text{exp}}$  are the experimental standard deviations in  $\Psi$  and  $\Delta$ , respectively, which were calculated from the known error bars on the calibration parameters and the fluctuation of the measured data over an averaged cycle of the rotating polarizer and analyzer. Equation (7) has  $2N$  and  $M$  in the prefactor, because there are two measured values included in the calculation for each  $\Psi$  and  $\Delta$  pair. The calculated data  $\psi_i^{\text{th}}$  and  $\Delta_i^{\text{th}}$  are generated by using the appropriate models as shown in Fig. 6 with corresponding dispersion relations [29].

The optical constants of the BVO films are obtained from spectroscopic ellipsometry measurements that are carried out at room temperature using an ellipsometer with variable-angle, synchronously rotating polarizers and analyzers. Figure 7a and b show the measured ellipsometric data ( $\Psi$  and  $\Delta$ ) and calculated results by the relaxed Lorentz model for the BVO films on Pt/Ti/SiO<sub>2</sub>/Si substrates in the ultraviolet–visible region. In order to estimate the optical constants of the BVO films, the ellipsometric spectra were analyzed by multilayer modeling in four layers. For this spectral range, the optical constants of the BVO films are mainly contributed by indirect transitions. Table 1 lists all the best-fit model parameters and the thicknesses of both the rough and the dense BVO layers. There is a good agreement between the measured data (circles) and the calculated data (line). The estimated thickness of 324 nm is in good agreement with the value obtained by cross-sectional scanning electron microscopy.

The refractive index and extinction coefficient of the BVO films obtained from the best-fit model are shown in Fig. 8a and b. The refractive index initially increases sharply and shows a maximum around 356 nm and then decreases rapidly with increasing wavelength. On the other hand, the extinction coefficient decreases rapidly with increasing wavelength up to 450 nm and subsequently remains almost constant. In the vis-

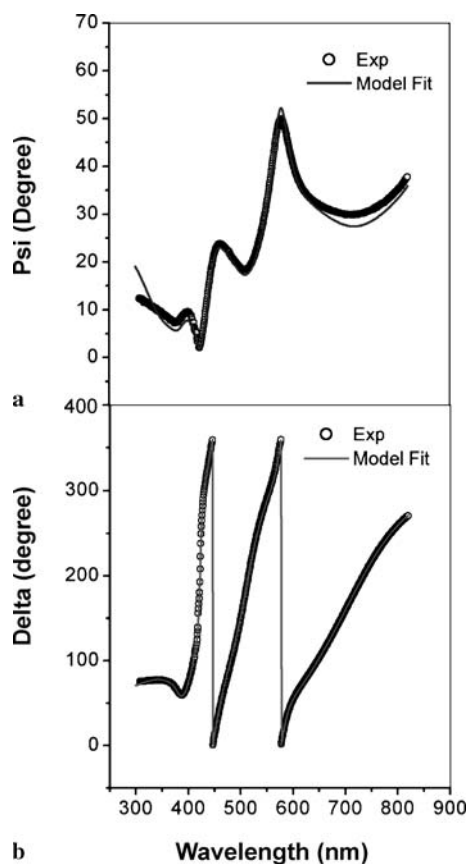


**FIGURE 7**  $\Psi$  and  $\Delta$  values in the 300–850 nm range for  $\text{Bi}_2\text{VO}_{5.5}$  films grown on platinized silicon substrates. The *solid lines* are the model fit data

Sample	$\varepsilon_\infty$	$d_{\text{film}}$ (nm)	$d_r$ (nm)	$F_v$	$\sigma^*$
BVO	2.93	324.37	17.39	0.85	0.91

\* A smaller value indicates a better fit

**TABLE 1** Fitting parameters of  $\text{Bi}_2\text{VO}_{5.5}$  film on platinized silicon substrate determined by spectroscopic ellipsometry measurement

Sample	$n$	$k$	$\alpha$ ( $\text{cm}^{-1}$ )
BVO (ellipsometry)	2.31	0.056	$7.4 \times 10^5$
BVO (transmission)	2.1	0.038	$8.7 \times 10^5$

**TABLE 2** The comparison of the optical constants of  $\text{Bi}_2\text{VO}_{5.5}$  thin films determined by ellipsometric and transmission studies

ible range (600 nm), the refractive index of the BVO film is about 2.31, with an extinction coefficient of 0.056. The optical constants of BVO films obtained from ellipsometric measurement analysis are in close agreement with those obtained from the transmission studies of the BVO thin films deposited on the Corning glass substrates (Table 2). However, a peak in the refractive index (Fig. 8a) that appears at 356 nm (3.47 eV) is likely to be arising from the indirect-band-gap transition. It may be noted that this value corresponds to a peak value in the ellipsometric angle  $\Delta$  appearing at the beginning of the interference oscillations.

The absorption coefficient ( $\alpha$ ) of the BVO films in the 300–820 nm range is shown in Fig. 9. It is observed that the absorption coefficient is quite high at the UV end and then

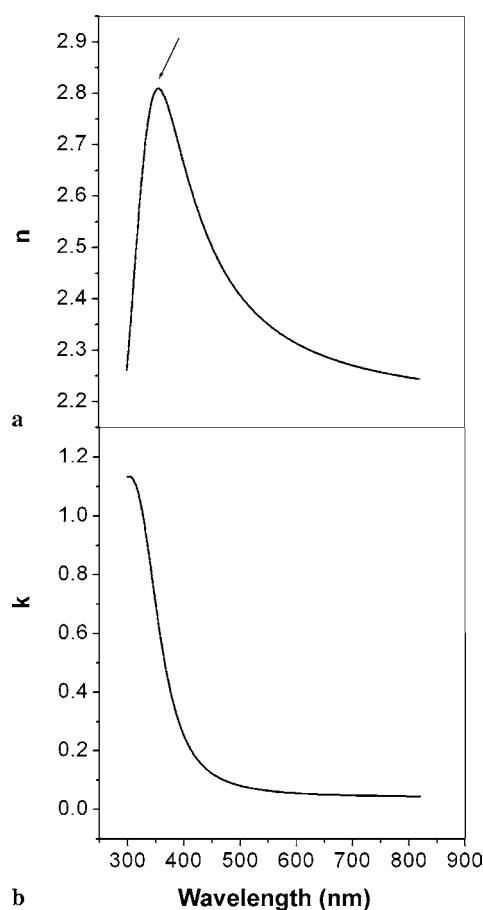


**FIGURE 8** The refractive index  $n$  and the extinction coefficient  $k$  of  $\text{Bi}_2\text{VO}_{5.5}$  film

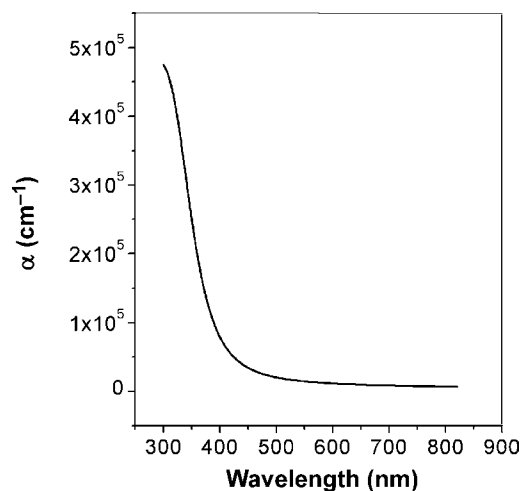


**FIGURE 9** The absorption coefficient  $\alpha$  of  $\text{Bi}_2\text{VO}_{5.5}$  film

it decreases sharply with increase in wavelength and the decrease is very insignificant subsequent to 550 nm.

#### 4 Conclusions

In conclusion, high-quality bismuth vanadate thin films have been fabricated on platinized silicon substrates by pulsed laser deposition. The BVO films were characterized by X-ray diffraction studies and the most pronounced

Bragg peaks were associated with (00 $l$ ) orientation. The microstructure of the films was analyzed by atomic force and scanning electron microscopy. The grain size was found to be in the range of 0.3–0.35  $\mu\text{m}$ , associated with a thickness of 325 nm. The value of the thickness of the films obtained from cross-sectional SEM agrees well with that obtained from ellipsometric data analysis. The BVO films exhibited good ferroelectric and dielectric properties. The polarization hysteresis ( $P$  vs.  $E$ ) studies of the BVO thin films at 300 K confirmed the remanent polarization ( $P_r$ ) and coercive field ( $E_c$ ) to be 9.3  $\mu\text{C}/\text{cm}^2$  and 365 kV/cm, respectively. The room-temperature dielectric constant and loss at 100 kHz were 130 and 0.04, respectively. The various models that were used for ellipsometric data analysis gave an excellent fitting to the experimental data. The optical constants,  $n \sim 2.31$  and  $k \sim 0.056$ , obtained at  $\lambda = 600$  nm were determined through multilayer analysis.

### REFERENCES

- 1 J.F. Scott, C.A. Paz de Araujo, *Science* **246**, 1400 (1989)
- 2 C.A. Paz de Araujo, J.D. Cuchiaro, L.D. McMillan, M.C. Scott, J.F. Scott, *Nature (London)* **374**, 627 (1995)
- 3 O. Auciello, J.F. Scott, R. Ramesh, *Phys. Today* **51**, 22 (1998)
- 4 P. Yang, N. Zhou, L. Zheng, H. Lu, C. Lin, *J. Phys. D* **30**, 527 (1997)
- 5 Y.H. Xu, J.D. Mackenzie, *Integr. Ferroelectr.* **1**, 17 (1992)
- 6 G.H. Haertling, *Ferroelectrics* **75**, 25 (1987)
- 7 M.P. Moret, M.A.C. Devillers, K. Wörthoff, P.K. Larsen, *J. Appl. Phys.* **92**, 468 (2002)
- 8 R. Watton, P. Manning, *Proc. SPIE* **3436**, 541 (1998)
- 9 C.M. Hanson, H.R. Beratan, J.F. Belcher, K.R. Udayakumar, K.L. Soch, *Proc. SPIE* **3379**, 60 (1998)
- 10 H. Xu, K. Hashimoto, T. Mukaigawa, H. Zhu, R. Kubo, T. Usuki, H. Kishihara, M. Noda, Y. Suzuki, M. Okuyama, *Proc. SPIE* **4130**, 140 (2000)
- 11 B.H. Park, B.S. Kang, S.D. Bu, T.W. Noh, J. Lee, M. Jo, *Nature (London)* **401**, 682 (1999)
- 12 H.N. Lee, D. Hesse, N. Zakharov, U. Gosele, *Science* **296**, 2006 (2002)
- 13 J.H. Bahng, M. Lee, H.L. Park, W. Kim, J.H. Jeong, K. Kim, *J. Appl. Phys. Lett.* **79**, 1664 (2001)
- 14 A. Kingon, *Nature (London)* **401**, 658 (1999)
- 15 B. Aurivillius, *Nature (London)* **2**, 519 (1950)
- 16 A.A. Bush, Y.N. Venevtsev, *Russ. J. Inorg. Chem.* **31**, 769 (1986)
- 17 V.G. Osipyan, L.M. Savchenko, V.L. Elbakyan, P.B. Avakyan, *Inorg. Mater.* **23**, 467 (1987)
- 18 V.N. Borisov, Y.M. Poplavko, P.B. Avakyan, V.G. Osipyan, *Sov. Phys. Solid State* **30**, 904 (1988)
- 19 K.B.R. Varma, G.N. Subbanna, T.N. Guru Row, C.N.R. Rao, *J. Mater. Res.* **5**, 2718 (1990)
- 20 K.V.R. Prasad, K.B.R. Varma, A.R. Raju, K.M. Satyalakshmi, R.M. Mal-lyya, M.S. Hegde, *Appl. Phys. Lett.* **63**, 1898 (1993)
- 21 Z. Huang, P. Yang, Y. Chang, J. Chu, *J. Appl. Phys.* **86**, 1771 (1999)
- 22 Z. Huang, X. Meng, P. Yang, Z. Zhang, J. Chu, *Appl. Phys. Lett.* **76**, 3980 (2000)
- 23 P. Yang, J. Xu, J. Ballato, R. Schwartz, D. Carroll, *Appl. Phys. Lett.* **80**, 3394 (2002)
- 24 A. Petraru, J. Schubert, M. Schmid, C. Buchal, *Appl. Phys. Lett.* **81**, 1375 (2002)
- 25 M. Viswanathan, G.K.M. Thutupalli, K.B.R. Varma, *Solid State Commun.* **98**, 535 (1996)
- 26 F.K. Lotgering, *J. Inorg. Nucl. Chem.* **9**, 113 (1959)
- 27 N. Kumari, S.B. Krupanidhi, K.B.R. Varma, *Mater. Sci. Eng. B* **138**, 22 (2007)
- 28 R.M.A. Azzam, N.M. Bashara, *Ellipsometry and Polarized Light* (North-Holland, Amsterdam, 1977)
- 29 Z.G. Hu, Z.M. Huang, Y.N. Wu, G.S. Wang, X.J. Meng, F.W. Shi, J.H. Chu, *J. Vac. Sci. Technol. A* **22**, 1152 (2004)
- 30 D.E. Aspnes, J.B. Theeten, F. Hottier, *Phys. Rev. B* **20**, 3292 (1979)
- 31 J.H. Weaver, *Phys. Rev. B* **11**, 1416 (1975)